Published in final edited form as:

Reprod Toxicol. 2014 November ; 49: 86–100. doi:10.1016/j.reprotox.2014.07.074.

PVP formulated Fullerene (C60) increases Rho-kinase dependent Vascular Tissue Contractility in Pregnant Sprague Dawley Rats

Achini K. Vidanapathirana[1], **Leslie C. Thompson**[1], **Erin. E. Mann**[1], **Jillian T. Odom**[1], **Nathan A. Holland**[1], **Susan J. Sumner**[2], **Li Han**[2], **Anita H. Lewin**[2], **Timothy R. Fennell**[2], **Jared M. Brown**[3], and **Christopher J. Wingard**[1]

[1]Department of Physiology, Brody School of Medicine, East Carolina University, 600, Moye Boulevard, Greenville, NC, 27834, USA

[2]Discovery Sciences, RTI International, Research Triangle Park, NC, 27709, USA

[3]Department of Pharmaceutical Sciences, Skaggs School of Pharmacy and Pharmaceutical Sciences, University of Colorado, CO, 80045

Abstract

Pregnancy is a unique physiological state, in which C60 fullerene is reported to be distributed in both maternal and fetal tissues. Tissue distribution of C60 differs between pregnant and non-pregnant states, presumably due to functional changes in vasculature during pregnancy. We hypothesized that, polyvinylpyrorrolidone (PVP) formulated C60 (C60/PVP) increases vascular tissue contractility during pregnancy by increasing Rho-kinase activity. C60/PVP was administered intravenously to pregnant and non-pregnant female Sprague Dawley rats. Vascular responses were assessed using wire myography 24 hours post-exposure. Increased stress generation was observed in uterine artery, thoracic aorta and umbilical vein. Rho-Rho-kinase mediated force maintenance was increased in arterial segments from C60/PVP exposed pregnant rats when compared to PVP exposed rats. Our findings suggest that intravenous exposure to C60/PVP during pregnancy increases vascular tissue contractility of the uterine artery through elements of Rho-Rho-kinase signaling during late stages of pregnancy.

Keywords

Vascular tissue contractility; pregnancy; uterine artery; umbilical vein; nanotoxicology; Rho-kinase pathway; polyvinylpyrorrolidone

Corresponding author: Christopher J. Wingard, Ph.D., Associate Professor, Department of Physiology, Brody School of Medicine at East Carolina University, 600 Moye Blvd, Brody 6N98, Greenville, NC, USA, 27834, Ph. +1-252-744-2804, Fax. +1-252-744-3460, wingardc@ecu.edu.

Conflicts of Interest

We declare that no actual or potential conflicts of interests were involved in the findings reported herein. The authors are responsible for the conclusions described in this article, which may not represent those drawn by the National Institute of Environmental Health Sciences, American Heart Association, The University of Colorado, East Carolina University or RTI International.

1. Introduction

A nano-object is a material with one, two, or three external dimensions in the size range from approximately 1 – 100 nm. These nanomaterials are manufactured in different forms and used in various commercial, biomedical and research technological applications. Fullerenes are carbon based nanoparticles comprised entirely of carbon, in the form of a hollow sphere composed of linked hexagonal carbon rings. C60 fullerenes are composed of 60 carbon atoms and have an average diameter of 0.7 – 1.0 nm. Engineered fullerenes and their derivatives are designed for various industrial and biomedical applications increasing the probability of occupational, therapeutic and/or environmental exposure. The unregulated exposure to engineered nanomaterials, like C60, may impact human health, much like that described for exposure to particulates in ambient air associated with adverse cardiovascular effects. However, there is less known of the effects of exposure to nanoparticles on vulnerable life stages such as pregnancy. Intratracheal delivery of C60 fullerene is reported to translocate through the alveolar capillary barrier by transcytosis [1], resulting in access to the vascular compartment and to their deposition in endothelial cells. Alternatively, fullerenes and their derivatives used for different biomedical applications such as drug/gene delivery and as contrast agents in diagnostic imaging [2, 3] may be introduced directly into the vascular compartment. While the site and extent of C60 distribution within the pulmonary and extra-pulmonary tissues depends on the size of particle agglomerates and route of exposure, once exposed and distributed into the circulation C60 has a very low clearance from the body, remaining in organs/tissues as long as 180 days post-exposure [4, 5]. Considering its size and penetrability to tissues and subcellular locations [6], C60 can potentially alter intracellular signaling pathways in cells associated with the vascular walls and impact vascular function.

The current evidence on toxicity of fullerenes and their derivatives on different cell types and tissues are controversial. Fullerene C60 has been described as a molecule with antioxidant properties (*i.e*. a free radical sponge) and as a pro-inflammatory agent [7–10]. A commonly used coating/suspension medium for C60 is polyvinylpyrorrolidone (PVP), a water soluble polymer reported to be physiologically inert [11], but the PVP-C60 combination is reported to be toxic in some studies [12]. Non-ionic surfactants such as Tween and Triton provide better solubilization efficacy than PVP for C60 in miceller solutions [13]. However, these agents are more toxic considering their use for intravenous delivery as they hamper the antioxidative properties of C60. We chose to formulate C60 with PVP for our exposure studies as reactive oxygen species quenching ability of C60 is maintained with PVP, despite the moderate solubilisation power [13]

With expanding use of C60 based products, it is essential to understand how C60 exposure could potentially influence maternal and fetal vascular tissue contractility, as they can be used to identify both adverse effects and new mechanisms that can be utilized for biomedical applications. Any such impact on vascular contractility can be crucial in life stages such as pregnancy as blood supply to fetus/es can be altered affecting intrauterine growth. Nanoparticle exposures in non-pregnant life stages are known to change vascular reactivity of different vascular beds [14, 15]. The extensive proliferative and remodeling environment within the uterine and placental vasculature, particularly during late stages of

pregnancy, may make this state more vulnerable to effects of nanoparticle exposure. Pregnancy is a unique physiological state in which the uterine vasculature undergoes outward hypertrophic remodeling influenced by both systemic hormonal changes and localized variations in uterine circulation, which are dependent on the vascular location and stage of pregnancy [16]. The normal physiological changes in uterine vasculature during pregnancy involve enhanced vasodilatation, mediated by augmented basal production of endothelium derived dilator factors including nitric oxide [16, 17]. In contrast, Rho kinase activity, a potent pro-contraction process [18] is diminished in normal pregnancy [19] and we suggest may be a potential target for explaining changes in the contractile responses of vessel tissues following nanoparticle exposure.

The evidence for ultrafine particulate matter exposure and its association with pregnancy induced hypertension and low birth weight [20, 21] suggest that nanoparticles such as C60 exposure may also have adverse effects on pregnancy as their smaller size and large surface area to mass ratio may increases the possibility of biological and chemical interactions within the vascular system. Following intravenous administration in pregnant rats carbon-14 labeled C60 was reported to distribute to both maternal and fetal organs [22] and such fetal distribution is also reported with maternal exposure to other nanoparticles [23, 24]. The Sumner *et al* study also reported differences in the distribution pattern of radiolabelled C60 between pregnant and non-pregnant life stages [22], which is presumed to be due to changes in vascular reactivity of various vascular beds during pregnancy. The distribution kinetics of nanoparticles can influence both maternal and fetal vascular function [25], embryogenesis, cellular signalling, inflammation, cell cycle, lipid metabolism [26] fetal growth and malformations [23]. The effects of C60 exposure on maternal/fetal vascular reactivity have not been extensively investigated despite the possibility of occupational, general environmental and therapeutic/diagnostic exposures during pregnancy.

Our interests were to identify how PVP formulated C60 (C60/PVP) exposure affects the vascular responses during pregnancy and whether the resulting changes could impact intrauterine fetal growth to identify the potential need of further developmental toxicity assessments of these nanoparticles. We hypothesized that exposure to PVP formulated C60 via intravenous administration would enhance the contractile responses of uterine and placenta derived blood vessels during pregnancy, potentially reducing fetal blood supply. In addition, we assessed the contribution of RhoA-Rho kinase pathway as a potential mechanism underlying the changes in maternal vascular tissue contractility following C60 exposure.

2. Methods and Materials

2.1. Characterization of nanoparticles and suspensions

C60 was commercially procured from Sigma-Aldrich (St. Louis MO, USA, Catalog# 379646) and formulated with polyvinylpyrorrolidone (PVP) (Sigma-Aldrich, St. Louis MO, USA; Catalog# 234257) at RTI International (Research Triangle Park, NC, USA). In order to enable the suspension of these non-functionalized hydrophobic particles in physiologically compatible media, they were formulated with PVP, as described previously [22, 27]. The hydrodynamic diameter (Z-average) and the zeta potential of the C60/PVP

dosing suspensions were determined using a Malvern Zetasizer NanoZS (Malvern Instruments, Worcestershire, UK) with a 633 nm laser source, a detection angle of 173 degree, and a clear disposable sample cell. DLS measurements were carried at 25 °C using the following protocol: 1) 1st size determination; 2) zeta potential measurement; 3) 2nd size determination. The time elapsed between the two size determinations was approximately 8 minutes and the average particle size was calculated by averaging 1st and 2nd measurement results. The hydrodynamic particle sizes were measured at following time points: 1) right after sample preparation; 2) 38 minutes after sample preparation (mimic sample dosing period). The measurement at 38 minutes after the preparation was done to confirm that the suspensions remained stable at the time of delivery to rats.

2.2. Sprague Dawley rats

Ten to twelve week old timed-pregnant and non-pregnant female Sprague Dawley rats were purchased from Charles River Laboratories (Raleigh, NC, USA) to study the effects of *in vivo* C60 exposure on dame vascular tissue contractility and the changes in the fetal weight. The determination of pregnancy was by observation of the vaginal plug, the plug date was considered to be day zero of gestation and the rats arrived in the animal facility within 9–12 days of gestation on set. All rats were individually housed under 12 h light/dark cycles with standard rat chow and water provided *ad libitum*. Body weights were monitored (two readings taken three days apart) during a one week acclimation in Department of Comparative Medicine's animal facility at East Carolina University (ECU) to ensure progression of the pregnancy. In our preliminary experiments, two gestational age groups were evaluated: gestational days (GD) 14–16 and GD 17–19, to represent the maternal early third trimester of a human pregnancy and the early fetal stage of the rodent pregnancy. Following a detailed regression analysis, significant changes in vascular reactivity with C60 exposure were seen only in the late gestational stage (GD 17 – 19) group and all subsequent studies were done on this late gestational age group. All studies were designed to investigate potential mechanism of vascular dysfunction associated with C60 exposure and not specifically to investigate longitudinal or ontological change of the vascular with gestation. In addition, a third group composed of age-matched non-pregnant Sprague Dawley was also studied. All animal handling procedures were approved by ECU Institutional Animal Care and Use Committee.

2.3. C60/PVP Exposure/dosing

We exposed the pregnant and non-pregnant rats with PVP formulated C60 through intravenous administration, to study the effects of *in vivo* C60 exposure on vascular tissue contractility and on fetal growth. These rats were anesthetized using 2 – 3% isoflurane (Webster Veterinary, USA) dispersed in oxygen for all exposure procedures. Each exposure group: PVP formulated C60 (C60/PVP), PVP control or naïve group contained a minimum of eight animals. A dried aliquot of C60/PVP or PVP was resuspended in sterile 200 μl of 0.9% saline solution (0.9% w/v of NaCl, B. Braun Medical Inc., CA, USA) just before administration. The suspension was cup-horn sonicated for 2 minutes using a Misonix ultrasonic liquid processor at 65% amplitude at a total energy output of 10,817 joules (Model 1510R-MTH, Branson Ultrasonics Corp. Danbury, CT, USA). Twenty-four hours prior to sacrifice a suspension of C60/PVP (200 μl) containing 28 μg C60 (93.3 μg/kg body

weight) and 4.232 mg of PVP was administered intravenously through the tail vein using a 25G needle. Similarly, 200 μls of 1.4% PVP in saline (4.232 mg of PVP) was administered as vehicle control. Two groups of non-pregnant rats were also exposed to C60/PVP or PVP to determine effects of life stage on vascular reactivity. A set of pregnant and non-pregnant female rats of the same age, but not exposed to C60/PVP or PVP were used as naïve controls.

2.4. Blood pressure measurements

We assessed maternal blood pressure and resting heart rate in the C60/PVP or PVP exposed groups and in the naïve group to assess any systemic vascular effect resulting from the changes in vascular tissue contractility following *in vivo* C60 exposure. A CODA Monitor - non-invasive blood pressure system (Kent Scientific, CT, USA) with the tail-cuff was used to follow systemic blood pressure and heart rate changes while the rats were held in rodent restraining bags (AIMS Inc. USA), on a 37 °C heat pad without anesthesia. Rats were acclimated to the tail-cuff three days before blood pressure measurements to minimize changes in blood pressure and heart rate associated with the stress of handling. These measurements were carried out at GD 10 (*i.e*. mid-second trimester), before exposure and 24 hours post-exposure (*i.e*. immediately before sacrifice: GD 17–19, mid-third trimester). The mean of three readings from each animal at each time point was used for comparison.

2.5. Ultrasonography of the rat heart

The ejection fraction of the rat heart was assessed in C60/PVP or PVP exposed groups and in the naïve group to identify the presence of a cardiac effect contributing to the hemodynamic status, hence affecting the uterine fetal blood supply following *in vivo* C60 exposure. Two dimensional cardiac ultrasonography was performed under anesthesia with 2–3% isoflurane (Webster Veterinary, USA) dispersed in oxygen at GD 10, before exposure and 24 hours post exposure (i.e. immediately before sacrifice: GD 17–19) using Vevo 2100 High Resolution Imaging System (FujifilmVisual Sonics Inc. Toronto, Canada). Vevo 2100 PC Workstation Only-Version 1.1.2 software was used to calculate the ejection fraction using 2–3 images from parasternal long axis view of the heart at each time point and confirmed using the parasternal short axis view.

2.6. Tissue and sample collection

Twenty-four hours post-exposure, rats were anesthetized in a transparent receptacle containing gauze soaked with 70% isoflurane (Webster Veterinary, USA) in propylene glycol (Amersco, OH, USA). After induction of plane 3 level of anesthesia, the animals were subjected to a midline incision and euthanized by pneumothorax. One milliliter of blood was withdrawn directly from the maternal right ventricle. Fetal blood from each dam was collected from three fetuses from the left mid-uterine region, pooled and considered as one sample. Maternal and fetal serum were prepared by centrifugation of the whole blood (20,400 x *g* for 30 minutes at 4°C), snap frozen and stored at − 80 °C for subsequent cytokine analysis.

The two uterine horns with fetuses, small intestinal loop with superior mesenteric arcade and thoracic aorta were carefully excised without tension and placed in ice cold physiological

saline solution (PSS; mM) 140 NaCl, 5.0 KCl, 1.6 $CaCl_2$, 1.2 $MgSO_4$, 1.2 MOPS (3-[N-morpholino]-propane sulfonic acid), 5.6 D-glucose, 0.02 EDTA, at a pH of 7.4. Vascular segments of 0.5 – 2.0 mm length from the main uterine artery (diameter 150 – 300 μm), first order mesenteric artery (diameter 150 – 250 μm), and thoracic aorta (diameter 2 – 3 mm) were isolated and cleaned of adhering connective tissue and fat for isolated vessel studies with wire myography. Segments of the main uterine artery were isolated from the arterial loop supplying the left mid-uterine region, avoiding distal embryos to minimize site dependent changes in vascular reactivity [16]. Two umbilical veins (diameter 400 – 550 μm) from umbilical cords of different fetuses from the left mid-uterine region were isolated from each exposed/naive dam. Segments from the thoracic aorta and main uterine artery unused for vascular studies were snap-frozen and stored at – 80 °C for subsequent RNA, protein and histological analysis.

2.7. Bronchoalveolar lavage and lung histology

We used cell counts of bronchoalveolar lavage (BAL) fluid and lung histology to assess any pulmonary inflammatory response following exposure to C60, as a large proportion of nanoparticles are filtered in the lungs following intravenous exposure [4] with a life stage dependent variability [22]. BAL and cell counts were performed on rats 24 hours post-exposure as described by Wang *et al* [28]. Briefly, the right lung of each rat was lavaged *in situ* four times with ice-cold Hanks balanced salt solution (26.25 mL/kg body weight) and all BAL fluids were centrifuged. Then the total cells were counted, 20,000 cells were centrifuged using a Cytospin IV (Shandon Scientific Ltd., Cheshire, UK) and stained with a three-step hematology stain (Richard Allan Scientific, Kalamazoo, MI, USA). The differential cell count was determined by morphology, evaluating 300 cells per slide. The unlavaged left lung was fixed and stained for histology as described by Wang *et al* [28]. Briefly, the left lung was inflated with 10% neutral buffered formalin fixative for 24 – 72 hours, processed, embedded in paraffin and 5 μM sections were mounted on slides. The sections were stained with hematoxylin and eosin and evaluated using light microscopy.

2.8. Cytokine analysis

The serum cytokines can be elevated/deranged as a result of a systemic or local inflammatory response following nanoparticle exposure, contributing to the changes in vascular tissue contractility. Thus, selected serum cytokines and chemokines (IL6, IL10, TNFα, MCP1, PAI1, VEGF, INFγ, and IL1β) were assessed using Milliplex MAP Cytokine/Chemokine Panel and Immunoassay (EMD Millipore MA, USA). Serum cardiovascular disease markers (PAI1 and vWF) were assessed using Milliplex MAP Rat Cardiovascular Panel and Immunoassay (EMD Millipore MA, USA) from both maternal and fetal serum according to the manufacturer's directions. Assays were run using a Luminex 100/200 (Luminex, Austin, TX) and results reported using Luminex xPONENT® software versions 2.3/3.1.

2.9. Wire myographic studies

The changes in vascular tissue contractility following C60 exposure were assessed in the vessel segments isolated from C60/PVP or PVP exposed or naïve rats, using wire

myography. All vessel segments were mounted into a DMT 610M multi-channel myograph system (Danish Myo Technology, Aarhus N, Denmark) using 40 μm wires or pins and bathed in PSS bubbled with medical grade air at 37 °C. Optimal resting tension for each arterial vessel segment was established at 90% of internal circumference (IC) produced at tensions equivalent to 100 mmHg (13.3 kPa). Subsequently, segments that developed a stress response greater than 1 mN/mm^2 to a potassium depolarization (109 mM K^+ PSS with equal molar substitution for Na^+ with K^+) were considered viable. Endothelial function was assessed by pre-stimulating with 1.0 μM phenylephrine followed by 3.0 μM acetylcholine, an intact endothelium was considered present when the acetylcholine induced relaxation was >70% (>20% for uterine vessels) of the phenylephrine steady-state stress. All three arterial vessel preparations were then subjected to cumulative concentrations of phenylephrine (0.001 – 30 μM), endothelin-1 (0.0001 – 1 μM) and acetylcholine (0.0001 – 30 μM). Cumulative concentration responses to angiotensin II (0.0001 – 0.1 μM) and serotonin (0.001 – 1 μM) were studied for uterine and mesenteric arteries respectively. The force generated by each vessel segment at each concentration was recorded and normalized to surface area to calculate the active stress generated in response to the stimuli. Cumulative concentrations of the Rho-kinase inhibitor HA1077 (0.001 – 10 μM) were applied to arterial segments during phenylephrine pre-contraction in order to identify the contribution of Rho-kinase activity in mediating changes in the contractile response following C60/PVP exposure.

The umbilical vein carries blood from the placenta to the fetal circulation and we chose the umbilical vein to assess the changes in tissue contractility that may be directly affecting the fetal blood supply. Following equilibration, umbilical vein segments were stretched and set to an IC equal to 90% of the IC when the wall tension is equivalent to 20 mmHg (5.1 kPa) [29]. As these vessel segments are reported to not respond to most agonists [29], viability was assessed using K^+PSS, pre-contracted with thromboxane-mimetic U46619 (1 μM) and subjected to cumulative concentrations of acetylcholine (0.0001 – 30 μM), followed by 1 μM sodium nitroprusside.

2.10. mRNA and protein analysis in aortic tissue homogenates

Aortic tissue homogenates from the thoracic aortic samples collected 24 hours post-exposure to C60/PVP or to PVP were utilized for mRNA and protein analysis of the key components of the RhoA/Rho kinase (ROCK) pathway. Half of the stored thoracic artery segments were homogenized in Trizol reagent (Invitrogen Corp. Grand Island, NY, USA) using a Minibeads Beater (Biospec Products, Bartlesville, OK, USA). The total mRNA was extracted, converted to cDNA and Real-Time PCR was done using primers for *RhoA*, *ROCK1, ROCK2* and *eNOS*. The fold changes in the expression were calculated using the ΔΔCt method as described previously [30]. The fold changes were calculated in comparison to naïve controls of pregnant and non-pregnant rats, following normalization to either of two housekeeping genes: *GAPDH* and *ACTB* (β actin). The other half of the samples was homogenized using a glass motor and pestle on ice with T-Line Laboratory Stirrer (Talboys Engineering Corp. Thorofare, NJ, USA) with a modified radioimmunoprecipitation assay (RIPA) buffer at a ratio of 10 μl buffer /mg tissue weight. Protein concentration in the homogenate was determined using the Bradford Protein Assay (Bio Rad, Hercules, CA,

USA) and read using a Bio-Tek Synergy HT microplate reader with Gen 5 software (Bio-Tek Instruments, Winooski, VT). Equal protein quantities from each sample were used for a 96-well ROCK Activity Assay (Cell Biolabs Inc. San Diego, CA, USA), carried out according to the manufacturer's instructions.

2.11. Cell culture, mRNA and protein quantification

The endothelial cells are the innermost lining of the vascular tissue and may come in contact with nanoparticles following their distribution in blood [4]. Thus, *in vitro* studies were done using rat aortic endothelial cells (RAEC) to identify the contribution of the endothelial Rho mediated signaling in changing the vascular tissue contractile responses. RAEC were purchased from Cascade Biologics (Eugene, OR, USA) and grown with Dulbecco's Modified Eagle Medium (DMEM). RAEC cultures at >90% confluence were treated with C60/PVP over a 1–10 μg/cm^2 dose range for 2–12 hours. Cell viability was assessed using MTS assay and live-dead cell assay [30]. Real time PCR was done as described previously [30] to identify any changes in *Rho A, ROCK1* and *ROCK2* mRNA. In-Cell Western Assay (Li-Cor Biosciences, Lincoln, NE, USA) was performed following 12 hour *in vitro* exposure to C60/PVP or PVP to assess the changes in target protein expression [31]. Briefly, the treated cells were immediately fixed with 3.7% formaldehyde with 1X PBS, permeabilized with 0.1% Triton-X, blocked with Odyssey blocking buffer (LI-COR Biosciences, Lincoln, NE, USA), and treated with RhoA (1:1000), ROCK1 (1:500), ROCK2 (1:500) and eNOS (1:1000) primary antibodies (Santa Cruz Biotechnology Inc., USA and Cell Signaling Danvers, MA, USA). IRDye 800CW Secondary Antibodies (LI-COR Biosciences, Lincoln, NE, USA) were used in 1:10000 dilution for target proteins and DNA were stained with DRAQ5 and Sapphire 700 (Cell Signaling, Danvers, MA, USA) for cell number normalization. The fluorescence was detected, quantified and analyzed using Li-Cor Odyssey Infrared Imaging System and software.

2.12. Measurement of the fetal parameters

The body weights of pregnant dams were recorded just before sacrifice and the litter size was recorded before the uterine vessel isolation. Three fetuses from each dam were isolated from the right mid-uterine region, to be consistent with the isolation of uterine and umbilical vessel segments. The individual fetal weights were measured using Ohaus Explorer Analytical Balance (Ohaus Corporation, NJ, USA) to assess effects of maternal C60 exposure on the fetal weight gain. The placentae attached to these fetuses were also weighed. Both fetuses and placentae were observed for gross morphological abnormalities.

2.13. Statistics

GraphPad Prism 5 software (San Diego, CA) was used for statistical analysis. Data are presented as mean ± SEM (standard error of mean) and differences were considered statistically significant if $p < 0.05$. Repeated measures analysis of variance (ANOVA) [32] and Bonferroni post hoc test were used to compare the concentration/dose responses. Each concentration response curve was also compared across treatment groups using a regression analysis by examining the best-fit value [32]. EC_{50} values for concentration responses in myographic studies were calculated using the Hill equation. For agonists with biphasic

responses (endothelin-1 and angiotensin II) EC_{50} values were calculated only for the contraction phase. Relaxation phase was considered separately and percentage of relaxation from the maximum stress was compared using a two-tailed t test. A two-tailed t test was used compare mean EC_{50}, umbilical vein stress generation, fetal/placental weight, mRNA, protein and cytokine expression levels between different treatment groups.

3. Results

3.1. Particle size distribution and zeta potential

The zeta potentials of both PVP and C60/PVP suspensions were within the range of 0.8 −1.5 mV for all samples, indicating low suspension stability. Particle size data presented as intensity based hydrodynamic diameter (z-average) and second order polydispersity index (PDI), obtained by using CONTIN algorithm, for both PVP and C60/PVP saline suspensions show good agreement between triplicates as well as between size measurements over a 38 minute time period for saline suspensions of both C60/PVP and PVP (Supplementary Table 1). A decrease in the number of large particles was observed in the intensity based size distribution between measurements #1 and #2 (data not shown). A homogenous stable C60 dosing solution is required to understand the effect of C60 on vascular responses of pregnant and non-pregnant rats. The inherent insolubility of C60 in physiologically compatible media has led to the development of various dispersal methods for C60 applications *in vitro* and *in vivo*. These include the use of polymers, surfactants, cyclodextrin, liposome, solvent exchange or nanomilling [33–39]. We opted to utilize a suspension of polymer-wrapped C60 using polyvinylpyrrolidone (PVP), since PVP is often considered biologically compatible, being used as a plasma expander, as a binder and most recently having been approved for use in cosmetics [39–41]. As indicated by the measured zeta potential, the C60/PVP suspension was inherently unstable. However, the minimal change in the polydispersity index, suggests reasonable homogeneity in the size distribution within the suspension. A decrease in the intensity-based number of larger diameter particles after 38 minutes (data not shown) of the suspension could not be accounted for as agglomeration of suspended particles, but may be explained by gravitational forces which removed larger particles from the active measurement area. Despite these physical effects on measurements over the time span to generate and deliver the suspension, the average particle size remained within 0.5% of the mean size determination. The average particle diameter was determined for our suspension (370 nm) using a 29 kDa PVP and is in reasonable agreement with the diameter reported for the C60/PVP complex Radical Sponge® (680 nm) using the 60–80 kDa PVP [42].

3.2. Maternal blood pressure, heart rate and ejection fraction

The resting systolic, diastolic, mean blood pressures, heart rate and calculated ejection fraction at GD 10, immediately before intravenous exposure and 24 hours post-exposure are reported in Table 1. The differences of these parameters between pre- and post- exposure were not statistically significant.

3.3. Maternal serum cytokine analysis

The mean values of maternal serum cytokines 24 hours following exposure to C60/PVP or PVP are reported in Table 2. The mean MCP1 level in the naïve pregnant rats was 65% lower than the naïve non-pregnant rats and was also relatively low with PVP (by 78.5%) or C60/PVP (by 63.6%) in the pregnant rats when compared to the non-pregnant rats with the same exposure. Similarly, the mean levels of TNFα were reduced in the naïve (by 83.4%) and PVP (by 81.7%) in the pregnant group when compared to the non-pregnant. The IFNγ level was reduced by 73.5% in the pregnant group following C60/PVP exposure. The mean VEGF level was 8.5 fold higher in the naïve pregnant rats compared to the non-pregnant.

3.4. Maternal Bronchoalveolar Lavage (BAL) cell counts and histology

The number of macrophages in the BAL cell counts was increased in the pregnant rats following exposure to PVP (115.3%) or C60/PVP (92.5%) and was also relatively higher than in the corresponding exposure groups of non-pregnant rats (see Supplementary Figure 1).

3.5. Responses of arterial segments 24 hours post-exposure to C60/PVP

3.5.1. Main uterine artery—Twenty-four hours following C60/PVP exposure there was 2.8 mN/mm^2 (55.3%) increase in the maximum stress generating ability in response to phenylephrine in the uterine artery segments when compared to PVP exposed segments (Figure 1.A) in the pregnant group. A similar pattern of response with ~1 mN/mm^2 increase in the force generation capacity was seen for endothelin-1 (22.5%, Figure 1.C) and angiotensin II (29%, Figure 1.E) stimulation without changes in EC_{50} (Supplementary Table 2). The overall stress generation ability of the uterine vessel segments from naïve pregnant animals was smaller than those vessels from naïve non-pregnant animals. The myographic assessment of uterine arterial segments from non-pregnant female rats revealed no differences in the responses following C60/PVP or PVP exposure (Figure 1.B, D, F and H).

Relaxation responses from the peak force generated at higher concentrations of endothelin-1 were 13.7 ± 2.2% for C60/PVP, 21.8 ± 3.9% for PVP and 31.29 ± 12.29 % for naïve. Relaxation responses from the peak force generated at higher concentrations of angiotensin II were 33.3 ±11.3 % for C60/PVP, 37.4 ± 5.3% for PVP and 30.3 ± 10.1% for naive. The relative relaxation (%) to acetylcholine under 30 μM phenylephrine pre-contraction was not affected by C60/PVP, but the calculated EC_{50} value increased by 156% suggesting that a higher concentration of acetylcholine was needed to generate the relaxation response following C60/PVP exposure (Figure 1.G and Supplementary Table 2).

3.5.2. First order mesenteric artery—The stress generation in response to phenylephrine, endothelin-1 and serotonin stimulation of mesenteric artery segments from pregnant animals was not different between C60/PVP or PVP exposed groups (Figure 2.A, C and E). The contractile responses in the mesenteric artery segments from pregnant animals were diminished by ~50% in both PVP and C60/PVP groups for endothelin 1 (49.6% with PVP and 61.7% with C60/PVP) and serotonin (41.3% with PVP and 46.9% with C60/PVP) when compared to the naïve controls (Figure 2.C and E). The overall stress generation of mesenteric artery segments to stimulation from pregnant animals was smaller than from

non-pregnant animals. The only difference in the contractile responses in vessel segments from non–pregnant animals was seen with endothelin-1 stimulation with ~ 16% increase in the maximum stress generation following C60/PVP or PVP exposure (Figure 2.B, D, F and H).

The relaxation response at higher concentrations of ET-1 were attenuated for C60/PVP 19.5 ± 4.1 %, PVP 25.1 ± 7.2 % as compared to the naïve 58.7 ± 13.4 % group. The relaxation response to acetylcholine was increased in the vessel segments from PVP exposed rats when compared to vessel segments from C60/PVP exposed rats by 9.6 % in pregnant group and by 19.9% in non-pregnant group (Figure 2.G and H).

3.5.3. Thoracic aorta—The maximum stress generation in response to phenylephrine (0.001 – 10 μM) was 15.7% larger in the C60/PVP exposed segments when compared to PVP (Figure 3.A). Similarly, the endothelin-1 mediated stress generation was 19.4% greater following C60/PVP exposure when compared to either PVP or naïve controls in the pregnant rats (Figure 3.C). The relaxation response to acetylcholine (0.001 – 10 μM) were not different between PVP and C60/PVP exposed and naïve thoracic aortic segments (Figure 3.E). No differences were detected in non-pregnant thoracic aortic segments following C60/PVP or PVP exposure (Figure 3.B, D, and F).

3.6. Contribution of Rho-kinase activity on the vascular tissue contractility

3.6.1. Maintenance of stress in the presence of Rho kinase inhibitor—The segments of the main uterine artery from pregnant rats exposed to C60/PVP required higher concentrations of the Rho-kinase (ROCK) inhibitor, HA1077 to maximally relax a phenylephrine pre-contraction as the C60/PVP exposed segments relaxed 30.8% less than the PVP and 15.0% less than the naïve controls at the highest HA1077 concentration (Figure 4.A and E). Similarly, the maximum relaxation was 18.4% less in the C60/PVP group compared to the naïve segments of the thoracic aorta from pregnant rats. In contrast with these contractile responses, the mesenteric vessel segments, exposed to C60/PVP had ~24% greater relaxation responses to the mid-range concentrations of HA1077 as compared to responses of segments from PVP and naïve controls, but these differences were not statistically significant (Figure 4.C). The only differences seen in the responses of vessel segments from non-pregnant rats were the 8.0 % lower relaxation with C60/PVP and 13.0% lower with PVP when compared to the naïve, at highest concentrations of HA1077 in uterine artery segments (Figure 4.B, D and F).

3.6.2. RhoA, ROCK expression and activity in aortic tissue homogenates—*RhoA, ROCK1* and *ROCK2* mRNA expression levels from the C60/PVP groups were not significantly increased in aortic tissue homogenates when compared to PVP groups in both pregnant and non-pregnant rats. However, the overall fold changes for these targets when compared to the naïve controls were higher in the pregnant group (data not shown). No significant changes were seen in the total ROCK activity of aortic tissue homogenates following C60/PVP treatment as assessed by the ROCK activity assay (data not shown).

3.6.3. RhoA, ROCK mRNA and protein expression in rat aortic endothelial cells—The cell viability was not changed following *in vitro* exposure to C60/PVP or PVP (data not shown). Cell viability was not changed following *in vitro* exposure of rat aortic endothelial cells to C60/PVP or PVP (data not shown). The mRNA expression of *RhoA, ROCK1, ROCK2* and *eNOS* was not significantly changed in RAEC with 2–12 hour treatment with C60/PVP when compared to PVP treated samples (data not shown). However, the protein expression was increased for RhoA (26.4%), ROCK2 (52.1%) and eNOS (28.1%) with 12 hours *in vitro* exposure to 10 μg/cm^2 C60/PVP as assessed by the In-cell Western Assay (Figure 5.A- D).

3.7. Changes in the fetal components following C60 exposure

3.7.1. Changes in umbilical vein contractility—The contractility of the umbilical vein was assessed in C60/PVP or PVP exposed and naïve fetuses. The stress generation was increased by 65.5% in the presence of K^+PSS and by 65.8% in the presence of 1 μM of the thromboxane mimetic (U46619) in umbilical vein segments from C60/PVP exposed rats when compared to the PVP controls (Figure 6.A). These vessels did not display any response to acetylcholine. The relaxation response to 1 μM SNP with a stable U46619 pre-contraction was diminished by 9.49% in the C60/PVP exposure group, but was not statistically significant (Figure 6.B).

3.7.2. Changes in the fetal and placental weight—Since there is a significant weight gain in naïve fetuses during each day of gestation, we have reported the weights after re-grouping them according to GD at sacrifice. Mean weights of pregnant dams at the time of sacrifice, the mean litter size and range were not significantly different between treatment groups (Supplementary Table 3). We did not observe any gross external morphological abnormalities in the fetuses or placentae. Mean fetal weights from the C60/PVP exposed group and controls are reported in Figure 6.C while the placental weights are in Figure 6.D. The fetal weight was reduced in the C60/PVP exposed group by 12.1% compared to the PVP exposed group and by 16.0% compared to the naïve group on GD 19.

3.7.3. Fetal serum cytokine analysis—The serum cytokines of pooled fetal serum are reported in Table 3. The mean levels of cytokine of IL1β and IFNγ were increased in the fetal serum samples (86.0% and 322.9% compared to naïve) following maternal PVP exposure but were reduced (by 43.4% and 31.3% compared to naive) with maternal C60/PVP exposure.

4. Discussion

Our hypothesis that an increase in the contractile response of the main uterine artery and thoracic aorta following intravenous exposure to PVP formulated C60 (C60/PVP) would occur during late stages of pregnancy was supported by the main observation in this study. In addition, we found a concomitant increase in stress generation of the umbilical vein associated with a reduction in fetal weight supporting a suggestion that exposure to C60 fullerene during pregnancy may negatively impact fetal development by altering vascular supply to the fetus. However, we also found a profound PVP induced dilator effect, which

was as large in magnitude as the C60 contractile effect. Underpinning the increased stress generation ability was evidence for increased involvement of Rho-kinase signaling in C60/PVP exposed vessel segments, suggesting a possible mechanism underlying the changes in vascular tissue response following C60/PVP exposure. To our knowledge, this is the first study to assess the effects of C60 on altering vascular tissue contractility during pregnancy by intravenous route of administration.

We were specifically interested in understanding how the vascular responses were sensitive to changes in life stage (*i.e*. pregnancy) as meditated by the Rho signaling pathway and chose to investigate the pharmacological responses of vascular segments from different vascular beds, by exposure to a single dose (93.3 μg/kg, 28 μg/rat) of this C60/PVP formulation. Previous studies have shown that intratracheal instillation of 100 μg (3–4 times higher than the dose we have used intravenously) of C60 in rats resulted in a pulmonary burden half-life of about 15 days [43] with minimal pulmonary inflammation 3 days after exposure [44] and evidence suggesting extra pulmonary translocation [1]. When C60 was administered intravenously to male rats once per day for four days (approximately 929 μg of C60 total), C60 accumulation in the lungs was evident from 1 day post-exposure out to 28 days post-exposure [4]. Compared to the above and to other studies [12, 22, 23] the dose we used is relatively low and is more representative of an acute exposure. The intravenous route was chosen to mimic a therapeutic exposure to C60 and also to assess the translocation effects on the cardiovascular system following pulmonary exposure. The choice of a 24 hour post-exposure time point was based on the consideration of reported distribution and clearance of nanoparticles which most often occurs within that time frame [4, 45] and provides a reasonable time to assess the vascular effects following acute exposure. Additionally, with a gestational period of 20 – 22 days in rats 24 hour accounts for approximately 5% of total gestation, a time frame in which fetal growth and organogenesis is significant. We recognize that due to the complexity of the study, there are limitations of using a single dose/time point in toxicological studies. Future detailed time and/or dose-response studies will have to be carried out to evaluate appropriate endpoints for incorporation of these findings into risk assessment. Caution must be used when interpreting our conclusions as this study was focused on examining a potential mechanism of enhanced vascular responsiveness following C60 exposure and not designed to investigate the longitudinal ontological changes in placental or fetal vascular development but these should be subject of future investigations.

Several changes in the abundance of circulating cytokines may have contributed to the vascular responses observed during pregnant and non-pregnant life stages by either PVP or C60/PVP. The suppression of inflammatory cytokines in the naïve pregnant group may be due to overall suppressed immune responses mediated by pregnancy related hormones [46]. These baseline differences are consistent even after the exposure to PVP or C60/PVP suggesting that the variances observed are largely due to physiological differences in the life stage rather than the exposure to nanomaterials. The increase in pro-inflammatory agent TNFα and endothelial derived pro-thrombotic agent PAI1 levels within the pregnant group following C60/PVP exposure suggests the initiation of an endothelium mediated

inflammatory response that may be contributing to an enhanced vascular contractile response.

Kubota *et al* examined the biodistribution of C60 in rats after tail vein administration and the highest C60 concentration was observed in the lungs, followed by spleen, liver, kidneys, and brain [4]. Similarly, Sumner *et al* reported that 26.4% of ^{14}C labelled C60 distributed in the lungs of the lactating dam, which was significantly higher than in the pregnant dam [22]. These results suggested that C60 injected in the tail vein could be filtered by lung capillary vessels and accumulate in the lungs in a life stage dependent manner, prior to being distributed to other tissues. Thus we chose to assess the responses of the lungs following C60 exposure as such responses can contribute to changing vascular tissue contractility through inflammatory agents and autonomic responses [47]. Macrophages were increased in BAL fluid during pregnancy following exposure to PVP, which was further increased following C60/PVP exposure. We believe that this type of response would support an increased reactivity of the innate immune barriers [46] associated with higher pathogenic susceptibility during pregnancy. In contrast, the unchanged eosinophil count suggests that these responses to PVP and C60/PVP exposure are a protective; particle engulfment based responses rather than a hypersensitivity reaction. Our findings are in agreement with others that have reported activation of alveolar macrophages and presence of cytokines as a clearance response to pulmonary exposure to C60 [5, 8] and other nanoparticles [48]. These cellular responses were highest at 24 hours post exposure and waned over the course of 7 days [48]. Even following intravenous delivery most of the nanoparticles are expected to be filtered and retained in the lungs and liver [22], resulting in profiles of cell differential and cytokine expression that may be similar to those from a direct pulmonary exposure. These phenomena may be recapitulated with regard to the presence of inflammatory cells following intravenous C60/PVP exposure seen in our study.

Apart from the indirect effects mediated through pulmonary inflammation and circulating cytokines, there may also be direct effects of C60 on the vascular contractile responses as suggested by the increase in stress generation following intravenous nanoparticle administration. When compared to the naïve, it is evident that PVP alone reduced the stress generating response, which is reversed and augmented by C60/PVP combination bringing it closer to the naïve conditions. However, a clear vehicle vs. C60 toxicity effect cannot be easily addressed due to the insolubility of pristine C60 and we were unable to measure the stress generation induced by C60 alone. It has been reported that the differences in permeation of the lipid bilayer by C60 and its derivatives lead to different toxicity profiles [49]; non-derivatized C60 aggregates are considered more toxic [50]. Possibly hydroxylated fullerenes (fullerenols), which are water soluble and less toxic, might be useful alternatives in biomedical applications to eliminate vehicle induced effects associated with C60/PVP use during pregnancy.

We observed that the uterine arteries of naïve pregnant rats produced relatively lower stress generation when compared to the naive non-pregnant vessel segments. Within the pregnant group, exposure to C60/PVP increased stress generation in the uterine artery generating a response profile similar to that of the naïve non-pregnant state. The overall changes in vascular contraction were smaller in the non-pregnant rats following intravenous C60/ PVP

administration suggesting a higher susceptibility to changes by C60/PVP exposure in the pregnant state. Additionally, these changes were further confined to the late gestational stage (GD 17 – 19) as rats examined in our preliminary studies in the earlier gestational days (GD 14 −16) showed no C60 exposure induced effects. The large variation in the uterine artery responses could be attributed to the limitations of sample size of the analyzed vessels (after applying the cut-off values for the quality controls) and rapid changes in maternal physiology across the GD 17–19. The alternative approach was to use a single gestational day for exposure, which would be difficult to determine with the current evidence and would not be realistic considering the translational applications of the study. We did not observe significant differences of the mesenteric artery segments suggesting the low sensitivity of the mesenteric vascular bed to C60 when compared to uterine vasculature during pregnancy. A possible explanation for the different vascular bed responses may be related to changes in vascular remodeling [51] and the expression of mediators such as PPARγ during pregnancy that are known to influence contractile responses of the two vascular beds [52].

Our data suggest that intravenous C60/PVP exposure during pregnancy increases the vascular contractile response of the uterine artery to several agonists including phenylephrine, endothelin 1 and angiotensin II. Similar responses were seen with the thoracic aorta suggesting a common contractile regulatory pathway involved in the C60/PVP exposure. The RhoA-Rho kinase (ROCK) pathway is such a regulatory process associated with the various agonists investigated in this study [53]. ROCK activity may be contributing in several ways to increase the contractile response in VSMC such as regulation of intracellular calcium and changing the phosphorylation status of the MLCP [53]. Several observations in our study support the hypothesis of an increase in ROCK activity. C60/PVP exposure sensitizes the contractile response to both phenylephrine and endothelin-1 and manifests as augmented stress generation in uterine and thoracic aorta preparations. Secondly, the relaxation response of C60/PVP exposed vessel segments to ROCK inhibitor HA1077 was attenuated. While HA1077 may also inhibit other protein kinases, it is believed that it selectively inhibits ROCK in the concentration range used in this study [54]. Thirdly, PAI1, a circulating endothelial derived pro-thrombogenic agent which is associated with RhoA-ROCK expression in the endothelial cells [55] was increased following C60/PVP exposure. Alternatively, up regulation of RhoA and ROCK are also known to be associated with reduced expression/activation of endothelial nitric oxide synthase (eNOS) [56, 57], thereby reducing the relaxation response leading to enhanced contraction. In this study, we observed minor differences in acetylcholine mediated eNOS dependent relaxation in the isolated vessels. However, the mRNA and protein activity of RhoA, ROCK1 and ROCK2 in the aortic tissue homogenates did not significantly increase following C60/PVP exposure. The sample size, post-exposure time points examined, sample storage, limitations of the assays, post-transcriptional and post-translational modifications of these proteins could have contributed to these discrepancies. In the *in vitro* studies with RAEC, RhoA and ROCK 2 were increased in a manner complimentary to the responses seen in isolated vessels. The increase in the eNOS levels in RAEC may be a compensatory response to PVP or C60/PVP mediated via the other pathways in the endothelial cells. Based on all these observations, we can hypothesize that the Rho-ROCK pathway contributes to the changes in vascular tissue

contractility though PAI1 signaling and that the endothelial cells responds to C60 exposure by increasing RhoA, ROCK 2 and eNOS expression.

Although overall systemic effects of exposure to C60/PVP on blood pressure and cardiac output were not evident, the significant increase in contractile responses in uterine and umbilical vasculature could have negative implications on fetal blood supply, which was supported by the measured reduction in fetal weight particularly towards later gestation periods. This observation is significant in the context of developmental toxicity, as it may be a manifestation of impaired fetal growth, metabolism and organ development, considering that the embryonic stage is complete in a rodent pregnancy by GD 12–14 and we are studying the early fetal stage at GD 17–19, which extends up to 3–4 postnatal weeks. Similar changes in fetal weight were reported following other nanoparticle exposures [23, 24] and higher doses of C60 exposure have demonstrated potential harmful effects on embryogenesis [12]. The reduction in fetal weight can also be independent of the blood supply and may be due to C60/PVP that is distributed in fetal organs [22]. Litter size and body weight of the dams were not different between naïve/exposed groups, therefore can be considered to have no effect on fetal weights reported in this study. The placental weight does not change significantly during late stages of pregnancy and the increase in weight on GD 17 could be attributed to placental edema as a result of the inflammatory response following particle exposure. However, the limited cytokine profile does not support a profound inflammatory response in the fetal side following C60/PVP exposure. The disparity between the cytokine concentrations of fetal and maternal serum could be due to the relatively higher hemo concentration in fetal blood and the use of a pooled fetal blood sample.

5. Conclusions

In conclusion, the findings we present suggest that intravenous exposure to PVP formulated C60 during late stages of pregnancy increases the vascular tissue contractile response of the main uterine artery through elements of Rho-Rho-kinase signaling. The concomitant increase in the contractile response of the umbilical vein leads to a reduction in fetal weight suggesting an intrauterine growth restriction during late stages of pregnancy. The results from this study also, highlight the importance of selecting the appropriate formulation/vehicle for nanoparticle/C60 delivery to target tissues in biomedical applications, minimizing the potential for unanticipated vascular effects during pregnancy. The findings of this study emphasizes the significance of further studying the toxicity of C60 formulations in the context of developmental toxicity, particularly on embryogenesis, organ development and congenital abnormalities focusing on early, mid and late stages of pregnancy, which may/may not be dependent on the vascular effects that we have reported.

Supplementary Material

Refer to Web version on PubMed Central for supplementary material.

Acknowledgements

We would like to thank Catherine O'Sullivan who prepared all the vials of C60 /PVP and PVP vehicle pellets, to Dr. Jonathan Shannahan for assistance in cytokine analysis and to Alyssa DaVolio for the assistance with the PCR. We are very grateful to Dr. Robert M. Lust and Shaun Reece for their guidance with cardiac ultrasonography. This project was funded by the National Institute of Environmental Health Sciences grant U19 ES019525 and an AHA Mid-Atlantic Affiliate pre-doctoral fellowship to AKV.

Abbreviations

5HT	serotonin
Ach	acetylcholine
ANG II	angiotensin II
BAL	bronchoalveolar lavage
C60	Fullerenes with 60 carbons
C60/PVP	polyvinylpyrorrolidone formulated C60
DBP	diastolic blood pressure
GD	gestational day
EF	ejection fraction
HR	heart rate
MBP	mean blood pressure
NP	non-pregnant
P	pregnant
PE	phenylephrine
PSS	physiological saline solution
PVP	polyvinylpyrorrolidone
RAEC	rat aortic endothelial cells
SBP	systolic blood pressure

Reference List

1. Naota M, Shimada A, Morita T, Inoue K, Takano H. Translocation pathway of the intratracheally instilled C60 fullerene from the lung into the blood circulation in the mouse: possible association of diffusion and caveolae-mediated pinocytosis. Toxicologic pathology. 2009; 37:456–462. [PubMed: 19346503]
2. Sitharaman B, Tran LA, Pham QP, Bolskar RD, Muthupillai R, Flamm SD, et al. Gadofullerenes as nanoscale magnetic labels for cellular MRI. Contrast Media Mol Imaging. 2007; 2:139–146. [PubMed: 17583898]
3. Sitharaman B, Zakharian TY, Saraf A, Misra P, Ashcroft J, Pan S, et al. Water-soluble fullerene (C60) derivatives as nonviral gene-delivery vectors. Mol Pharm. 2008; 5:567–578. [PubMed: 18505267]

4. Kubota R, Tahara M, Shimizu K, Sugimoto N, Hirose A, Nishimura T. Time-dependent variation in the biodistribution of C(6)(0) in rats determined by liquid chromatography-tandem mass spectrometry. Toxicology letters. 2011; 206:172–177. [PubMed: 21787853]
5. Shinohara N, Nakazato T, Tamura M, Endoh S, Fukui H, Morimoto Y, et al. Clearance kinetics of fullerene C(6)(0) nanoparticles from rat lungs after intratracheal C(6)(0) instillation and inhalation C(6)(0) exposure. Toxicol Sci. 2010; 118:564–573. [PubMed: 20864628]
6. Bakry R, Vallant RM, Najam-ul-Haq M, Rainer M, Szabo Z, Huck CW, et al. Medicinal applications of fullerenes. Int J Nanomedicine. 2007; 2:639–649. [PubMed: 18203430]
7. Dellinger A, Zhou Z, Lenk R, MacFarland D, Kepley CL. Fullerene nanomaterials inhibit phorbol myristate acetate-induced inflammation. Exp Dermatol. 2009; 18:1079–1081. [PubMed: 19555428]
8. Park EJ, Kim H, Kim Y, Yi J, Choi K, Park K. Carbon fullerenes (C60s) can induce inflammatory responses in the lung of mice. Toxicology and applied pharmacology. 2010; 244:226–233. [PubMed: 20064541]
9. Yamawaki H, Iwai N. Cytotoxicity of water-soluble fullerene in vascular endothelial cells. Am J Physiol Cell Physiol. 2006; 290:C1495–C1502. [PubMed: 16407415]
10. Oberdorster E. Manufactured nanomaterials (fullerenes, C60) induce oxidative stress in the brain of juvenile largemouth bass. Environmental health perspectives. 2004; 112:1058–1062. [PubMed: 15238277]
11. Liu X, Xu Y, Wu Z, Chen H. Poly(N-vinylpyrrolidone)-Modified Surfaces for Biomedical Applications. Macromol Biosci. 2012
12. Tsuchiya T, Oguri I, Yamakoshi YN, Miyata N. Novel harmful effects of [60]fullerene on mouse embryos in vitro and in vivo. FEBS Lett. 1996; 393:139–145. [PubMed: 8804443]
13. Torres VM, Posa M, Srdjenovic B, Simplicio AL. Solubilization of fullerene C60 in micellar solutions of different solubilizers. Colloids and surfaces B, Biointerfaces. 2011; 82:46–53. [PubMed: 20828997]
14. Cuevas AK, Liberda EN, Gillespie PA, Allina J, Chen LC. Inhaled nickel nanoparticles alter vascular reactivity in C57BL/6 mice. Inhal Toxicol. 2010; (22 Suppl 2):100–106. [PubMed: 21142798]
15. Nurkiewicz TR, Porter DW, Hubbs AF, Stone S, Moseley AM, Cumpston JL, et al. Pulmonary particulate matter and systemic microvascular dysfunction. Res Rep Health Eff Inst. 2011:3–48. [PubMed: 22329339]
16. Osol G, Mandala M. Maternal uterine vascular remodeling during pregnancy. Physiology (Bethesda). 2009; 24:58–71. [PubMed: 19196652]
17. Osol G, Barron C, Gokina N, Mandala M. Inhibition of nitric oxide synthases abrogates pregnancy-induced uterine vascular expansive remodeling. J Vasc Res. 2009; 46:478–486. [PubMed: 19204405]
18. Christ G, Wingard C. Calcium sensitization as a pharmacological target in vascular smooth-muscle regulation. Curr Opin Investig Drugs. 2005; 6:920–933.
19. Goulopoulou S, Hannan JL, Matsumoto T, Webb RC. Pregnancy reduces RhoA/Rho kinase and protein kinase C signaling pathways downstream of thromboxane receptor activation in the rat uterine artery. Am J Physiol Heart Circ Physiol. 2012; 302:H2477–H2488. [PubMed: 22542618]
20. Rudra CB, Williams MA, Sheppard L, Koenig JQ, Schiff MA. Ambient carbon monoxide and fine particulate matter in relation to preeclampsia and preterm delivery in western Washington State. Environmental health perspectives. 2011; 119:886–892. [PubMed: 21262595]
21. Kloog I, Melly SJ, Ridgway WL, Coull BA, Schwartz J. Using new satellite based exposure methods to study the association between pregnancy pm2.5 exposure, premature birth and birth weight in Massachusetts. Environ Health. 2012; 11:40. [PubMed: 22709681]
22. Sumner SC, Fennell TR, Snyder RW, Taylor GF, Lewin AH. Distribution of carbon-14 labeled C60 ([14C]C60) in the pregnant and in the lactating dam and the effect of C60 exposure on the biochemical profile of urine. Journal of applied toxicology : JAT. 2010; 30:354–360. [PubMed: 20063269]
23. Yamashita K, Yoshioka Y, Higashisaka K, Mimura K, Morishita Y, Nozaki M, et al. Silica and titanium dioxide nanoparticles cause pregnancy complications in mice. Nat Nanotechnol. 2011; 6:321–328. [PubMed: 21460826]

24. Ema M, Kobayashi N, Naya M, Hanai S, Nakanishi J. Reproductive and developmental toxicity studies of manufactured nanomaterials. Reprod Toxicol. 2010; 30:343–352. [PubMed: 20600821]
25. Stapleton PA, Minarchick VC, Yi J, Engels K, McBride CR, Nurkiewicz TR. Maternal engineered nanomaterial exposure and fetal microvascular function: does the Barker hypothesis apply? American journal of obstetrics and gynecology. 2013; 209 227.e1–11.
26. Jackson P, Hougaard KS, Vogel U, Wu D, Casavant L, Williams A, et al. Exposure of pregnant mice to carbon black by intratracheal instillation: toxicogenomic effects in dams and offspring. Mutation research. 2012; 745:73–83. [PubMed: 22001195]
27. Yamakoshi YN, Yagami T, Fukuhara K, Sueyoshi S, Miyata N. Solubilization of fullerenes into water with polyvinylpyrrolidone applicable to biological tests. Journal of the Chemical Society, Chemical Communications. 1994:517–518.
28. Wang X, Katwa P, Podila R, Chen P, Ke PC, Rao AM, et al. Multi-walled carbon nanotube instillation impairs pulmonary function in C57BL/6 mice. Particle and fibre toxicology. 2011; 8:24. [PubMed: 21851604]
29. Kusinski LC, Baker PN, Sibley CP, Wareing M. In vitro assessment of mouse uterine and fetoplacental vascular function. Reprod Sci. 2009; 16:740–748. [PubMed: 19443912]
30. Vidanapathirana AK, Lai X, Hilderbrand SC, Pitzer JE, Podila R, Sumner SJ, et al. Multi-walled carbon nanotube directed gene and protein expression in cultured human aortic endothelial cells is influenced by suspension medium. Toxicology. 2012; 302:114–122. [PubMed: 23026733]
31. Stone JD, Narine A, Shaver PR, Fox JC, Vuncannon JR, Tulis DA. AMP-activated protein kinase inhibits vascular smooth muscle cell proliferation and migration and vascular remodeling following injury. Am J Physiol Heart Circ Physiol. 2013; 304:H369–H381. [PubMed: 23203966]
32. Ludbrook J. Repeated measurements and multiple comparisons in cardiovascular research. Cardiovascular research. 1994; 28:303–311. [PubMed: 8174149]
33. Misirkic MS, Todorovic-Markovic BM, Vucicevic LM, Janjetovic KD, Jokanovic VR, Dramicanin MD, et al. The protection of cells from nitric oxide-mediated apoptotic death by mechanochemically synthesized fullerene (C(60)) nanoparticles. Biomaterials. 2009; 30:2319–2328. [PubMed: 19195698]
34. Kato S, Kikuchi R, Aoshima H, Saitoh Y, Miwa N. Defensive effects of fullerene-C60/liposome complex against UVA-induced intracellular reactive oxygen species generation and cell death in human skin keratinocytes HaCaT, associated with intracellular uptake and extracellular excretion of fullerene-C60. J Photochem Photobiol B. 2010; 98:144–151. [PubMed: 20060738]
35. Andrievsky GV, Kosevich MV, Vovk OM, Shelkovsky VS, Vahchenko LA. On the Production of an Aqueous Colloidal Solution of Fullerenes. J Chem Society, Chemical Communication. 1995:1281–1282.
36. Ungurenasu C, Airinei A. Highly stable C(60)/poly(vinylpyrrolidone) charge-transfer complexes afford new predictions for biological applications of underivatized fullerenes. J Med Chem. 2000; 43:3186–3188. [PubMed: 10956226]
37. Samal S, Geckeler K. Cyclodextrin-fullerenes: a new class of water-soluble fullerenes. Chem Commun. 2000; 13:1101.
38. Shinohara N, Matsumoto K, Endoh S, Maru J, Nakanishi J. In vitro and in vivo genotoxicity tests on fullerene C60 nanoparticles. Toxicology letters. 2009; 191:289–296. [PubMed: 19772904]
39. Xiao L, Aoshima H, Saitoh Y, Miwa N. The effect of squalane-dissolved fullerene-C60 on adipogenesis-accompanied oxidative stress and macrophage activation in a preadipocyte-monocyte co-culture system. Biomaterials. 2010; 31:5976–5985. [PubMed: 20488530]
40. Xiao L, Takada H, Maeda K, Haramoto M, Miwa N. Antioxidant effects of water-soluble fullerene derivatives against ultraviolet ray or peroxylipid through their action of scavenging the reactive oxygen species in human skin keratinocytes. Biomed Pharmacother. 2005; 59:351–358. [PubMed: 16087310]
41. Lens M. Use of fullerenes in cosmetics. Recent Pat Biotechnol. 2009; 3:118–123. [PubMed: 19519567]
42. Xiao L, Takada H, Gan X, Miwa N. The water-soluble fullerene derivative "Radical Sponge" exerts cytoprotective action against UVA irradiation but not visible-light-catalyzed cytotoxicity in human skin keratinocytes. Bioorg Med Chem Lett. 2006; 16:1590–1595. [PubMed: 16439118]

43. Shinohara N, Gamo M, Nakanishi J. Fullerene c60: inhalation hazard assessment and derivation of a period-limited acceptable exposure level. Toxicological sciences : an official journal of the Society of Toxicology. 2011; 123:576–589. [PubMed: 21856993]
44. Ogami A, Yamamoto K, Morimoto Y, Fujita K, Hirohashi M, Oyabu T, et al. Pathological features of rat lung following inhalation and intratracheal instillation of C(60) fullerene. Inhalation toxicology. 2011; 23:407–416. [PubMed: 21639709]
45. Oberdorster G, Sharp Z, Atudorei V, Elder A, Gelein R, Lunts A, et al. Extrapulmonary translocation of ultrafine carbon particles following whole-body inhalation exposure of rats. Journal of toxicology and environmental health Part A. 2002; 65:1531–1543. [PubMed: 12396867]
46. Kraus TA, Engel SM, Sperling RS, Kellerman L, Lo Y, Wallenstein S, et al. Characterizing the pregnancy immune phenotype: results of the viral immunity and pregnancy (VIP) study. J Clin Immunol. 2012; 32:300–311. [PubMed: 22198680]
47. Donaldson K, Duffin R, Langrish JP, Miller MR, Mills NL, Poland CA, et al. Nanoparticles and the cardiovascular system: a critical review. Nanomedicine (London, England). 2013; 8:403–423.
48. Bonner JC, Silva RM, Taylor AJ, Brown JM, Hilderbrand SC, Castranova V, et al. Interlaboratory Evaluation of Rodent Pulmonary Responses to Engineered Nanomaterials: The NIEHS Nano GO Consortium. Environmental health perspectives. 2013; 121:676–682. [PubMed: 23649427]
49. Qiao R, Roberts AP, Mount AS, Klaine SJ, Ke PC. Translocation of C60 and its derivatives across a lipid bilayer. Nano Lett. 2007; 7:614–619. [PubMed: 17316055]
50. Sayes CM, Marchione AA, Reed KL, Warheit DB. Comparative pulmonary toxicity assessments of C60 water suspensions in rats: few differences in fullerene toxicity in vivo in contrast to in vitro profiles. Nano Lett. 2007; 7:2399–2406. [PubMed: 17630811]
51. Dalle Lucca JJ, Adeagbo AS, Alsip NL. Influence of oestrous cycle and pregnancy on the reactivity of the rat mesenteric vascular bed. Human reproduction (Oxford, England). 2000; 15:961–968.
52. Gokina NI, Chan S-L, Chapman AC, Oppenheimer K, Jetton T, Cipolla MJ. Inhibition of PPAR? during Rat Pregnancy Causes Intrauterine Growth Restriction and Attenuation of Uterine Vasodilation. Frontiers in Physiology. 2013:4. [PubMed: 23404365]
53. Fukata Y, Kaibuchi K, Amano M. Rho-Rho-kinase pathway in smooth muscle contraction and cytoskeletal reorganization of non-muscle cells. Trends in Pharmacological Sciences. 2001; 22:32–39. [PubMed: 11165670]
54. Davies SP, Reddy H, Caivano M, Cohen P. Specificity and mechanism of action of some commonly used protein kinase inhibitors. Biochem J. 2000; 351:95–105. [PubMed: 10998351]
55. Nakakuki T, Ito M, Iwasaki H, Kureishi Y, Okamoto R, Moriki N, et al. Rho/Rho-kinase pathway contributes to C-reactive protein-induced plasminogen activator inhibitor-1 expression in endothelial cells. Arterioscler Thromb Vasc Biol. 2005; 25:2088–2093. [PubMed: 16123329]
56. Eto M, Barandier C, Rathgeb L, Kozai T, Joch H, Yang Z, et al. Thrombin suppresses endothelial nitric oxide synthase and upregulates endothelin-converting enzyme-1 expression by distinct pathways: role of Rho/ROCK and mitogen-activated protein kinase. Circ Res. 2001; 89:583–590. [PubMed: 11577023]
57. Ming XF, Viswambharan H, Barandier C, Ruffieux J, Kaibuchi K, Rusconi S, et al. Rho GTPase/Rho kinase negatively regulates endothelial nitric oxide synthase phosphorylation through the inhibition of protein kinase B/Akt in human endothelial cells. Mol Cell Biol. 2002; 22:8467–8477. [PubMed: 12446767]

Highlights (mandatory)

Highlights consist of a short collection of bullet points that convey the core findings of the article and should be submitted in a separate file in the online submission system. Please use 'Highlights' in the file name and include 3 to 5 bullet points (maximum 85 characters, including spaces, per bullet point). See the following website for more information http://www.elsevier.com/highlights

- Pregnant and non-pregnant SD rats were intravenously exposed to PVP formulated C60
- Contractile responses in the main uterine artery were increased during pregnancy
- Increased contractility was dependent on the RhoA-ROCK pathway in vascular tissue
- Contractile responses were also increased in the umbilical vein
- These vascular changes may deprive the fetal weight gain during late pregnancy

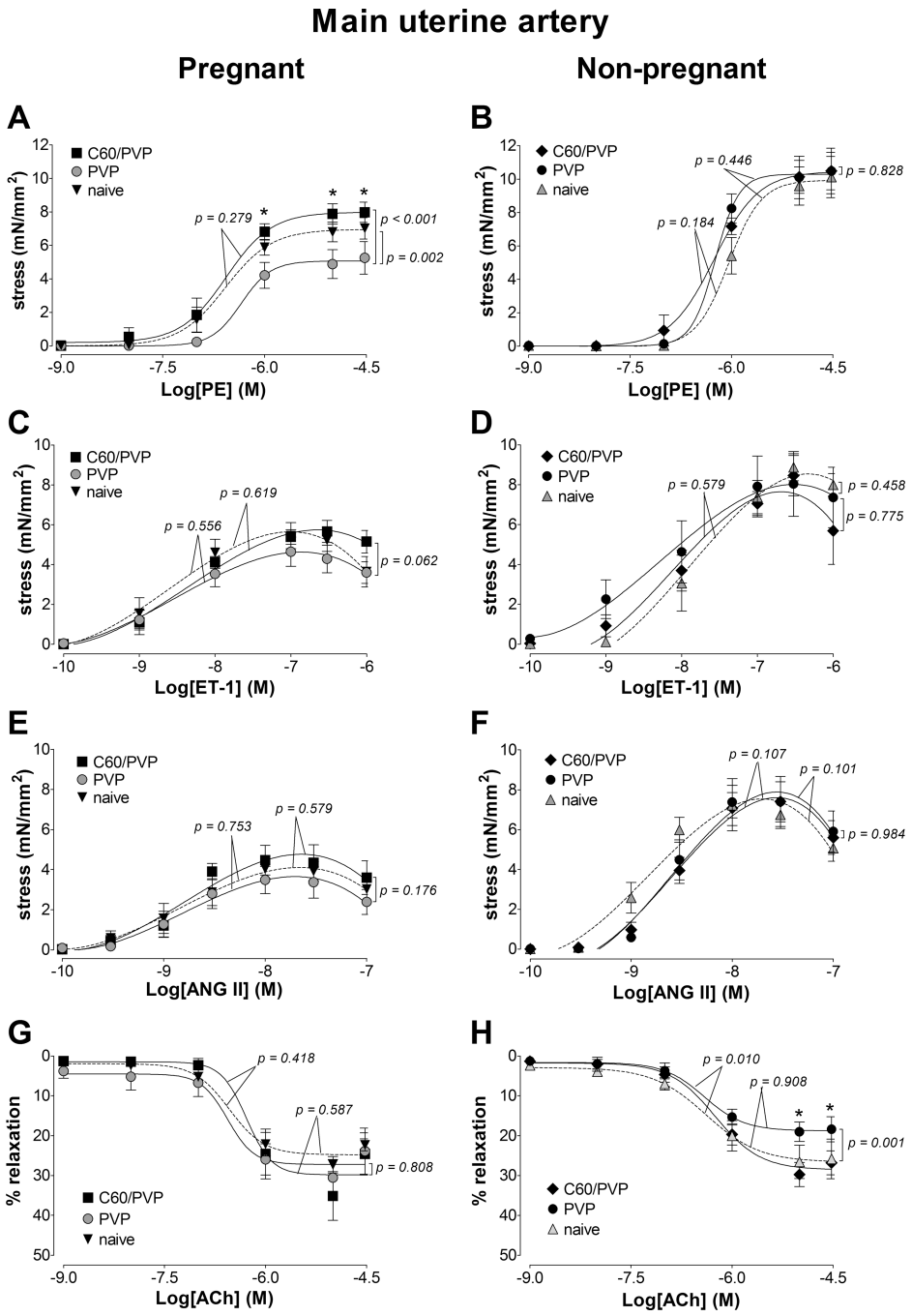

Figure 1. Changes in the contractile responses of the main uterine artery following exposure to C60/PVP

The changes in the contractile responses were assessed by wire myography of the main uterine artery 24 hours post-exposure to intravenous PVP formulated C60 (C60/PVP) or PVP from 17 −19 day pregnant (**A, C, E** and **G**) and non-pregnant female (**B, D, F** and **H**) Sprague Dawley rats. The stress generation in response to cumulative concentrations of phenylephrine (PE; **A** and **B**), endothelin 1 (ET-1; **C** and **D**) and angiotensin II (ANG II; **E** and **F**) are plotted. The percentage relaxation from a 30 μM phenylephrine pre-stimulation

stress level in response to cumulative concentrations of acetylcholine (Ach; **G** and **H**) is graphed. * indicates $p < 0.05$ compared to PVP using repeated measures ANOVA *(n = 4 – 8)*. The *p* values were derived following the comparison of each concentration response curve across treatment groups using a regression analysis by examining the best-fit value. The EC_{50} values and number of vessel segments for each concentration-response curve are included in Supplementary Table 2.

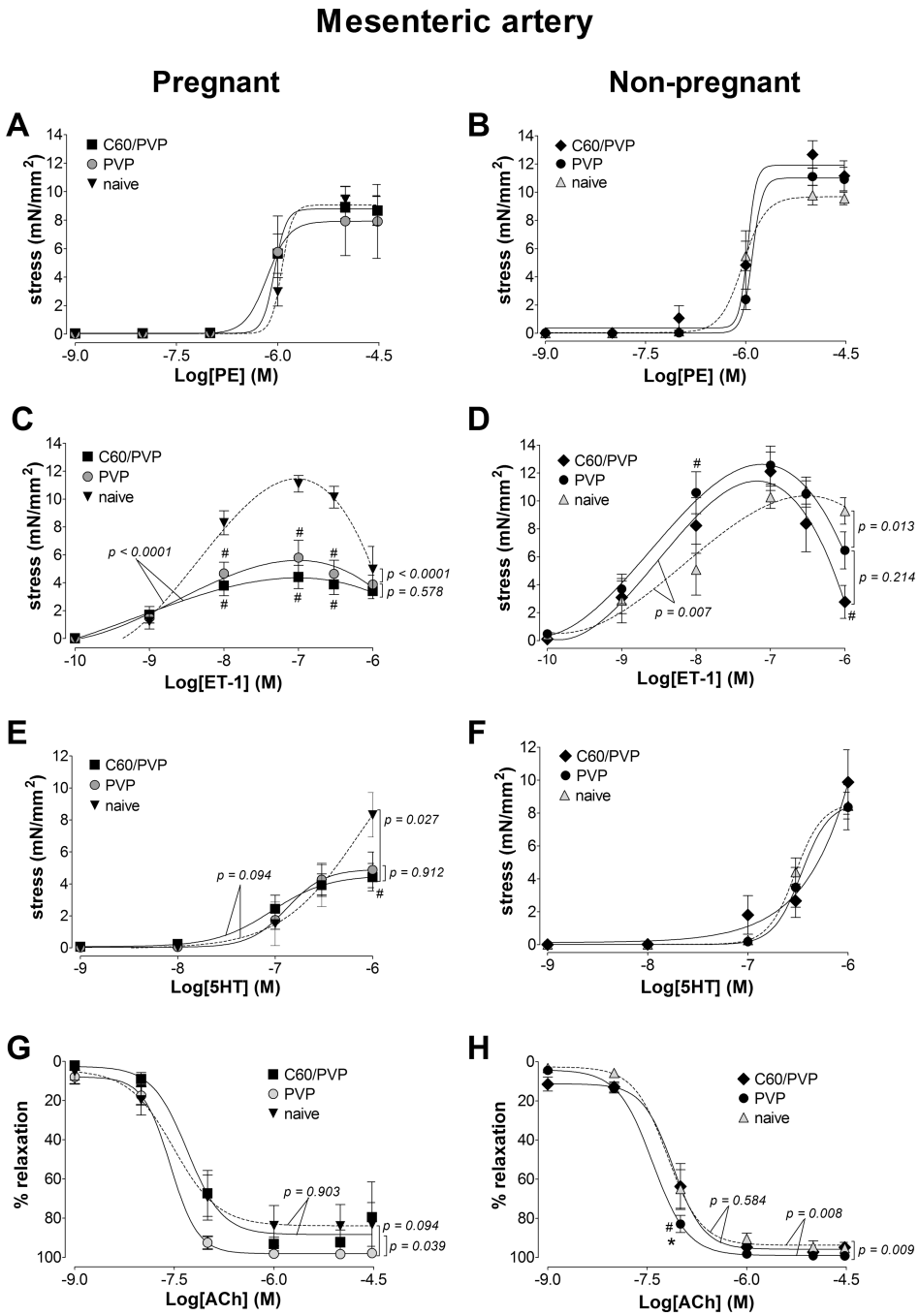

Figure 2. Changes in the contractile responses of the mesenteric artery following exposure to C60/PVP

The changes in the contractile responses were assessed by wire myography of the first order mesenteric artery 24 hours post-exposure to intravenous PVP formulated C60 (C60/PVP) or PVP from 17 – 19 day pregnant (**A, C, E** and **G**) and non-pregnant female (**B, D, F** and **H**) Sprague Dawley rats. The stress generation in response to cumulative concentrations of phenylephrine (PE; **A** and **B**), endothelin 1 (ET-1; **C** and **D**) and serotonin (5HT; **E** and **F**) are plotted. The percentage relaxation from a 30 μM phenylephrine pre-stimulation stress

level in response to cumulative concentrations of acetylcholine (Ach; **G** and **H**) is graphed. * indicates $p < 0.05$ compared to PVP while # indicates $p < 0.05$ compared to naïve using repeated measures ANOVA $(n = 4 – 8)$. The p values were derived following the comparison of each concentration response curve across treatment groups using a regression analysis by examining the best-fit value. The EC_{50} values and number of vessel segments for each concentration-response curve are included in Supplementary Table 2.

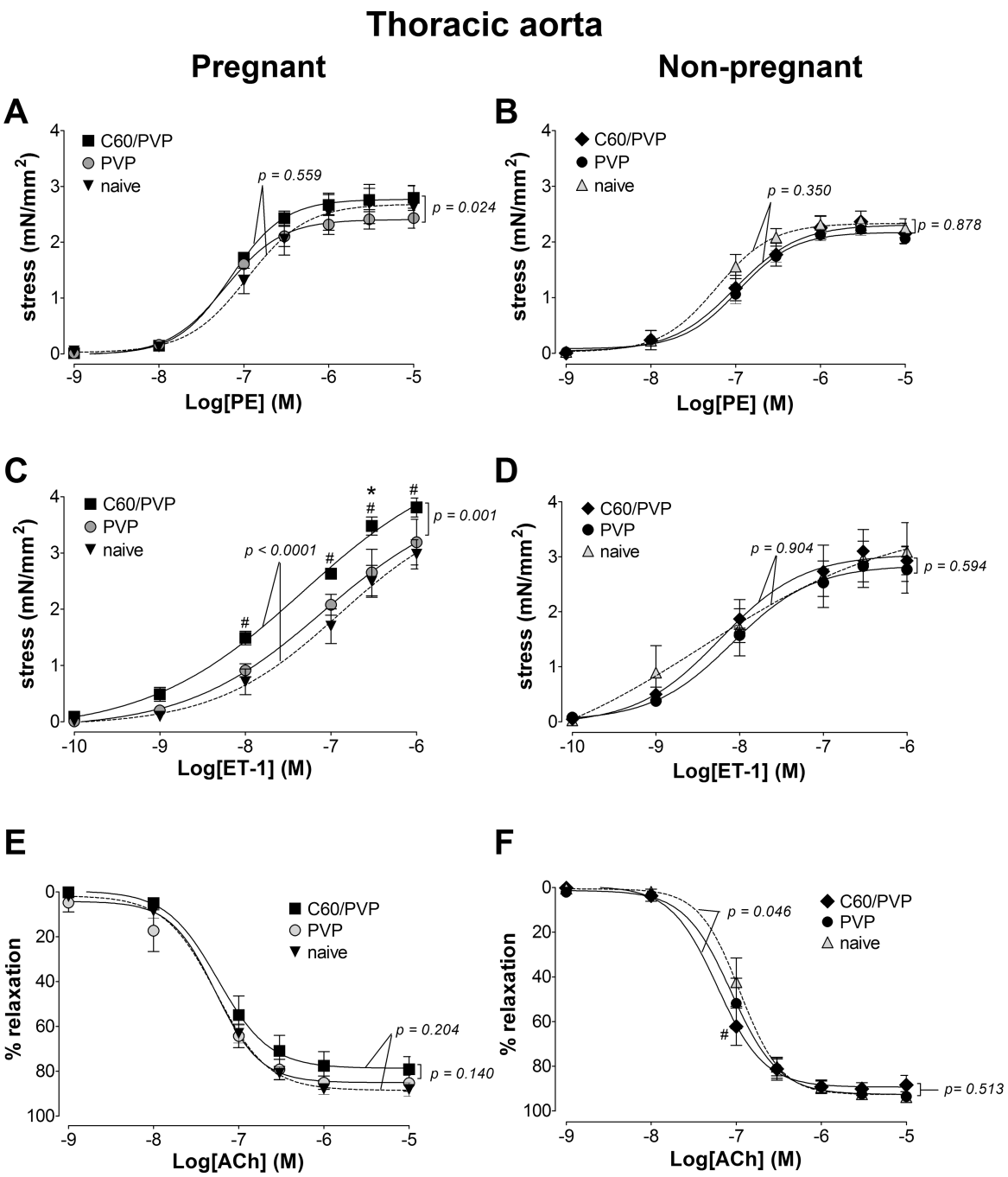

Figure 3. Changes in the contractile responses of the thoracic aorta following -exposure to C60/PVP

The changes in the contractile responses were assessed by wire myography in the thoracic aorta 24 hours post-exposure to intravenous PVP formulated C60 (C60/PVP) or PVP from 17 – 19 day pregnant (**A, C** and **E**) and non-pregnant female (**B, D** and **F**) Sprague Dawley rats. The stress generation in response to cumulative concentrations of phenylephrine (PE; **A** and **B**) and endothelin 1 (ET-1; **C** and **D**) are plotted. The percentage relaxation from a 10 μM phenylephrine pre-stimulation stress level in response to cumulative concentrations of

acetylcholine (Ach; **E** and **F**) is graphed. * indicates $p < 0.05$ compared to PVP while # indicates $p < 0.05$ compared to naïve using repeated measures ANOVA $(n = 4 – 8)$. The p values were derived following the comparison of each concentration response curve across treatment groups using a regression analysis by examining the best-fit value. The EC_{50} values and number of vessel segments for each concentration-response curve are included in Supplementary Table 2.

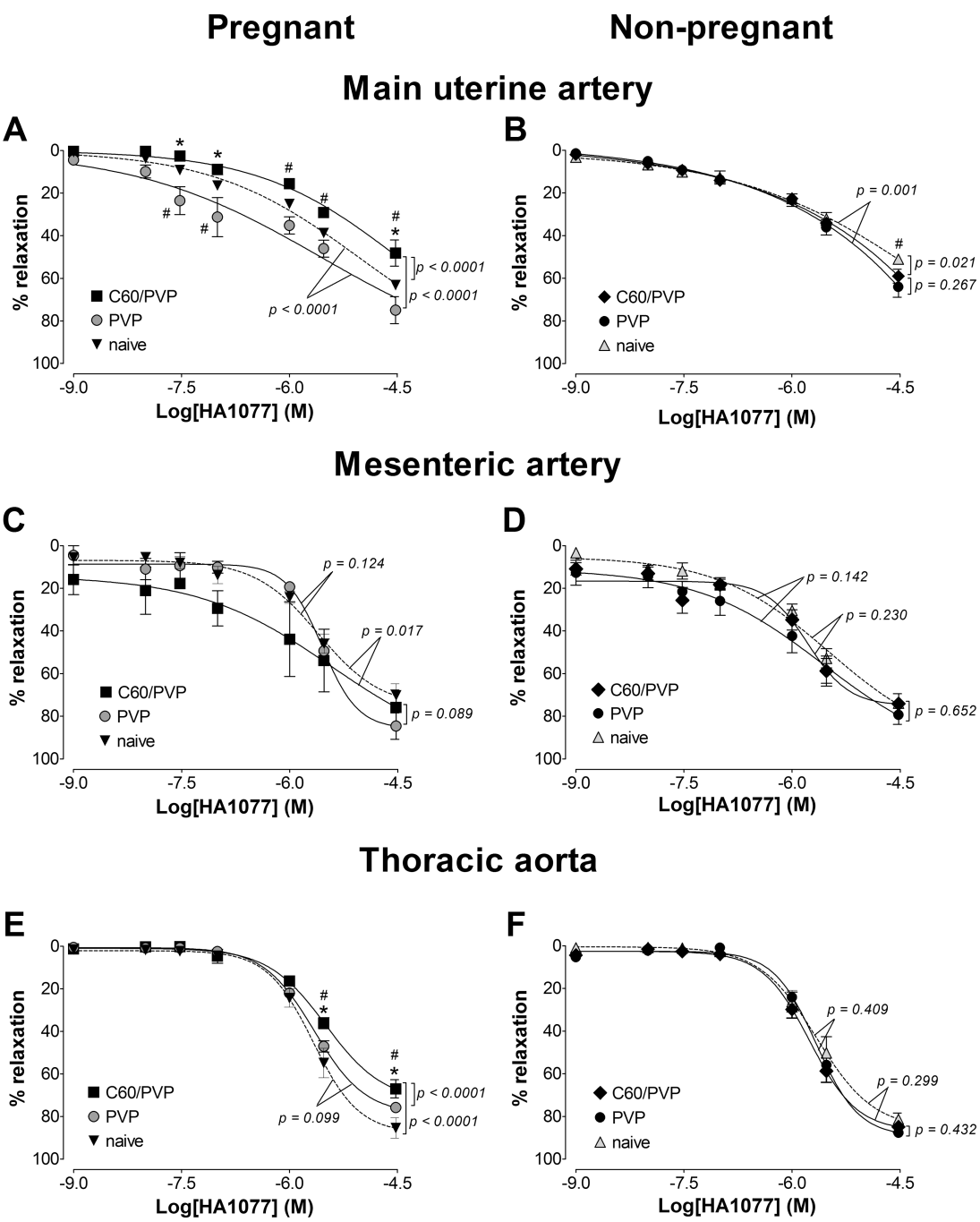

Figure 4. Changes in the stress generation in the presence of Rho-kinase inhibitor

The reduction in stress generation is reported as the percentage relaxation from a phenylephrine (30 μM for uterine/mesenteric arteries and 10 μM for aorta) pre-stimulation stress level in response to cumulative additions of a Rho kinase inhibitor (HA1077). These responses were assessed by wire myography 24 hours post-exposure to intravenous PVP formulated C60 (C60/PVP) or PVP from 17 – 19 days pregnant (**A, C** and **E**) and non-pregnant female (**B, D** and **F**) Sprague Dawley rats. **A** and **B:** main uterine artery; **C** and **D:** first order mesenteric artery; **E** and **F**: thoracic aorta. * indicates $p < 0.05$ compared to PVP

while # indicates $p < 0.05$ compared to naïve using repeated measures ANOVA $(n = 4 – 6)$. The p values were derived following the comparison of each concentration response curve across treatment groups using a regression analysis by examining the best-fit value. The EC_{50} values and number of vessel segments for each concentration-response curve are included in Supplementary Table 2.

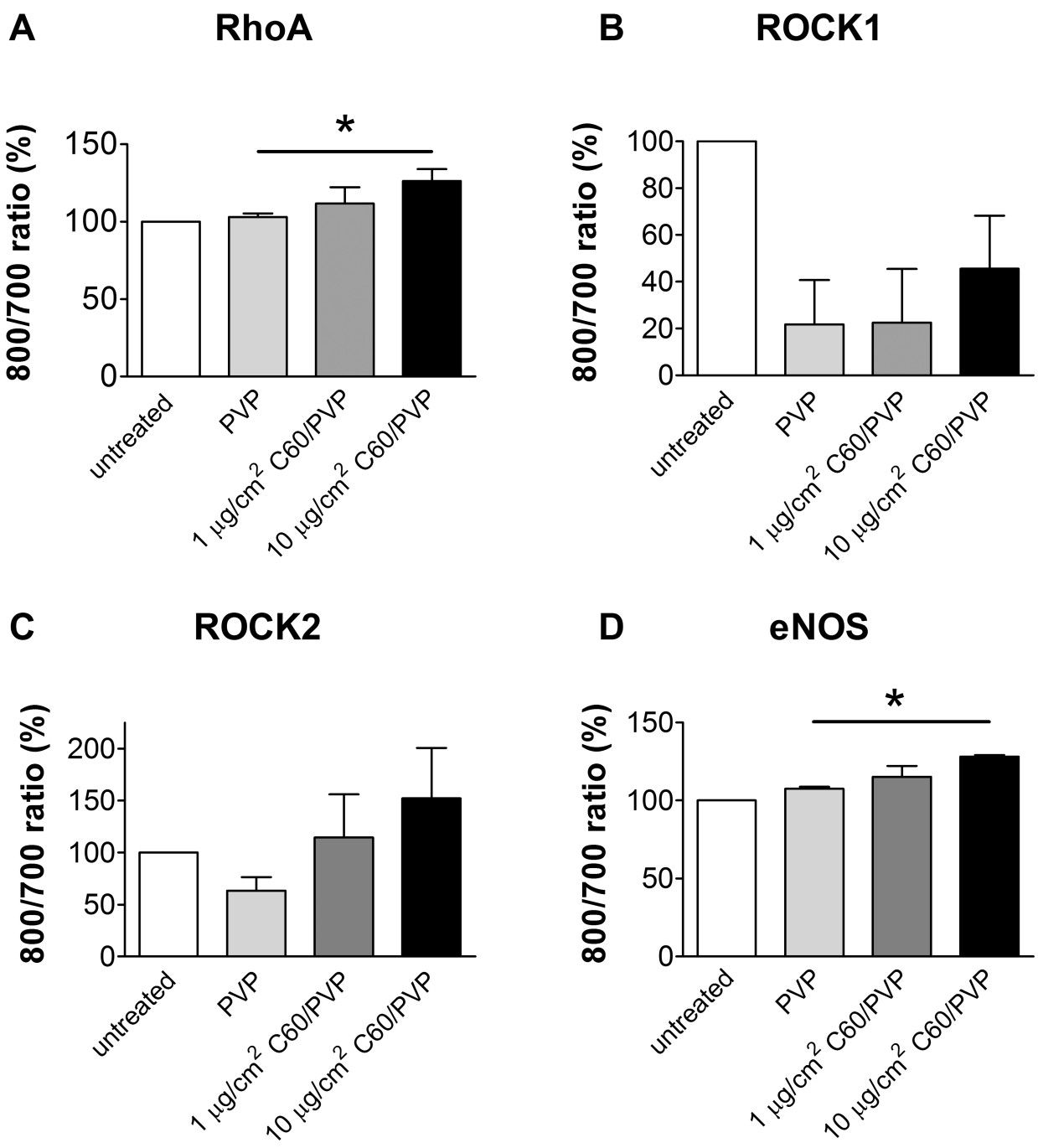

Figure 5. ROCK, RhoA and eNOS protein expression in rat aortic endothelial cells (RAEC) with 12 hours exposure to C60/PVP or PVP

RAEC were treated *in vitro* with C60/PVP at 1–10 μg/cm^2 concentration range for 12 hours. RhoA (**A**), ROCK1 (**B**), ROCK2 (**C**) and eNOS (**D**) expression was assessed by In-cell Western assay. The expression of the target proteins were normalized to the cell number and then normalized to the untreated control (considered as 100%). * indicates $p < 0.05$ when compared between the means (calculated using 3–5 independent experiments) of treatment groups using a two tailed t test

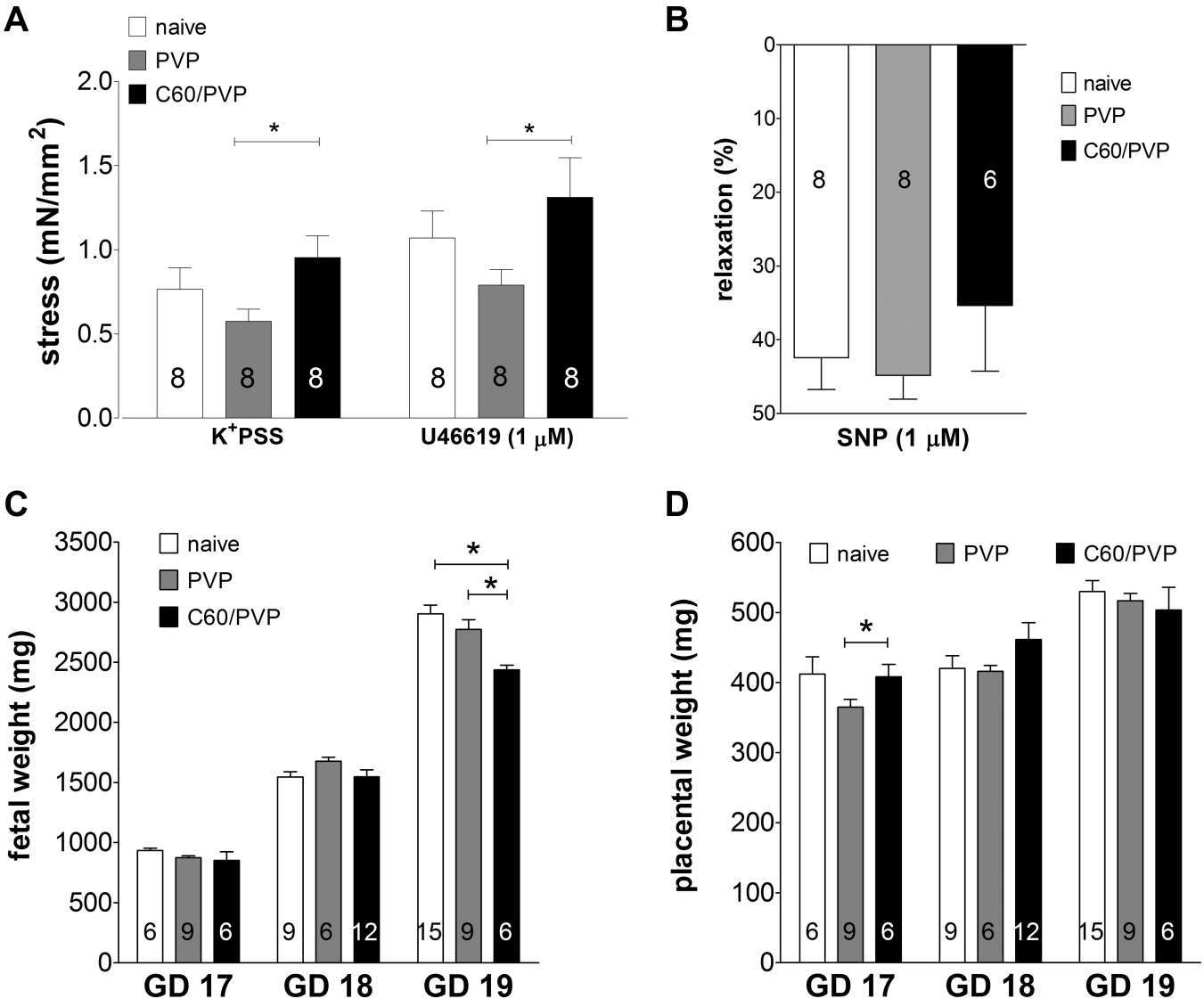

Figure 6. Changes in stress generation of the umbilical vein and fetal/placental weight following exposure to C60/PVP

A: changes stress generation as assessed by wire myography in response to K^+ depolarization (109 mM K^+ PSS) and thromboxane agonist (1 μM U46619) of the umbilical vein 24 h post-exposure to intravenous PVP formulated C60 (C60/PVP) or PVP from 17–19 days pregnant Sprague Dawley rats. **B:** percentage relaxation in response to sodium nitroprusside (1 μM SNP) following 1 μM U46619 pre-contraction . Changes in fetal **(C)** and placental **(D)** weight 24 hours post-exposure to intravenous C60/PVP or PVP from 17–19 days pregnant Sprague Dawley rats. * indicates $p < 0.05$ compared to PVP using a two tailed t test. The numbers inside the bars indicate the number of vessels/fetuses/placentae used for calculation of the mean.

Table 1
Cardiovascular parameters of pregnant Sprague Dawley rats

The mean and the SEM are reported *(n = number of pregnant rats)*.

	Time	Naive *(n = 5)*	PVP *(n = 4)*	C60/PVP *(n = 4)*
	GD 10	140.5 ± 9.3	130.8 ± 8.1	128.5 ± 8.7
SBP (mmHg)	Pre-exposure (GD 16–18)	154.7 ± 12.8	140.3 ± 11.3	160.3 ± 13.1
	Post-exposure (GD 17–19)	-	135.3 ± 16.9	145.5 ± 6.6
	GD 10	112.3 ± 6.0	100.3 ± 9.7	101.0 ± 9.5
DBP (mmHg)	Pre-exposure (GD 16–18)	125.8 ± 16.4	104.0 ± 14.1	107.0 ± 10.9
	Post-exposure (GD 17–19)	-	107.3 ± 18.9	110.8 ± 4.4
	GD 10	120.7 ± 6.4	110.0 ± 8.9	112.0 ± 9.9
MBP (mmHg)	Pre-exposure (GD 16–18)	135.1 ± 15.0	116.0 ± 13.2	136.8 ± 10.9
	Post-exposure (GD 17–19)	-	116.0 ± 18.3	124.0 ± 5.3
	GD 10	388 ± 11	388 ± 10	374 ± 5
HR (bpm)	Pre-exposure (GD 16–18)	390 ± 17	406 ± 22	375 ± 18
	Post-exposure (GD 17–19)	-	371 ± 37	390 ± 19
	GD 10	78.6 ± 2.5	78.1 ± 0.9	86.4 ±1.2
EF (%)	Pre-exposure (GD 16–18)	81.6 ± 1.2	80.8 ± 3.6	80.1± 2.5
	Post-exposure (GD 17–19)	-	80.8 ± 2.1	84.3 ±1.6

SBP: systolic blood pressure, DBP: diastolic blood pressure, MBP: mean blood pressure, HR: heart rate, EF: ejection fraction, GD: gestational day, GD 10: gestational day 10 (i.e. mid-second trimester), pre-exposure: just before intravenous administration of C60 or PVP, post-exposure: 24 h following exposure to intravenous C60/PVP or PVP (i.e. just before sacrifice)

Table 2

Cytokine levels in the maternal serum 24 hours post exposure to C60/PVP or PVP

The mean and the SEM are reported for maternal cytokines *(n = number of maternal serum samples analyzed)*.

Cytokine	NP-naive *(n = 8)*	NP- PVP *(n = 6)*	NP-C60/PVP *(n =6)*	P-naive *(n = 9)*	P- PVP *(n = 8)*	P-C60/PVP *(n = 8)*
IL1β (pg/ml)	56.0 ± 38.5	18.9 ± 8.2	22.4 ± 10.3	14.6 ± 7.1	4.5 ± 2.8	3.6 ± 2.4
IL6 (pg/ml)	1245.0 ± 826.0	50.2 ± 37.1	311.6 ± 149.9	77.9 ± 72.8	42.5 ± 36.3	57.1 ± 54.5
IL10 (pg/ml)	21.7 ± 9.0	3.8 ± 1.4	8.8 ± 3.3	5.8 ± 3.7	2.7 ± 2.7	2.3 ± 2.3
INFγ (pg/ml)	338.4 ± 135.3	148.8 ± 64.8	149.7 ± 38.9	198.5 ± 52.5	100.4 ± 53.9	52.7 ± 17.7$^{\#}$
MCP1 (pg/ml)	823.2 ± 223.9	445.8 ± 78.8	470.8 ± 66.4	288.1 ± 96.0†	95.9 ± 30.1†	171.4 ± 51.4†
VEGF (pg/ml)	53.7 ± 15.4	33.9 ± 6.7	33.9 ± 8.3	510.2 ± 111.9†	414.6 ± 96.8†	370.8 ± 124.0
TNFα (pg/ml)	40.9 ± 12.8	34.9 ± 3.6	34.5 ± 10.6	6.8 ± 3.9†	6.4 ± 3.4†	14.4 ± 5.6
PAI1 (pg/ml)	N/A	N/A	N/A	918.7 ± 222.6	1410.0 ± 63.7	1669.0 ± 240.1$^{\#}$
vWF(ng/ml)	N/A	N/A	N/A	236.6 ± 159.8	108.6 ± 101.2	144.1 ± 67.7

P = pregnant, NP = non-pregnant, N/A = not available

*indicates $p < 0.05$ when compared to PVP,

$^{\#}$indicates $p < 0.05$ when compared to naïve and

†indicates $p < 0.05$ when compared to same treatment in non-pregnant group.

Table 3

Cytokine levels in the fetal serum 24 hours post exposure to C60/PVP or PVP

The mean and the SEM are reported for fetal cytokines *(n = number of pooled fetal blood samples)*.

Cytokine	Naive *(n = 6)*	IV PVP *(n = 4)*	IV C60/PVP *(n = 4)*
IL1β (pg/ml)	1455.0 ± 372.5	2712.0 ± 610.9	794.2 ± 281.6*
IL6 (pg/ml)	75.7 ±16.8	1624.0 ± 979.8	82.59 ± 57.95
IL10 (pg/ml)	70.0 ± 17.0	584.4 ± 267.2	55.2 ± 17.0
INFγ (pg/ml)	283.3 ± 42.5	1198.0 ± 294.5#	194.7 ± 84.0*
MCP1 (pg/ml)	903.4 ± 310.8	1041.0 ± 215.7	721.9 ± 86.0
VEGF (pg/ml)	469.5 ± 83.0	557.7 ± 112.7	407.8 ± 33.3
TNFα (pg/ml)	5.9 ± 5.9	23.5 ± 19.5	8.4 ± 6.8

N/A = not available

* indicates $p < 0.05$ when compared to PVP while

# indicates $p < 0.05$ when compared to naïve.